Preparation, Characterization, and Water-Sorption Study of Polyvinyl Alcohol Based Hydrogels with Grafted Hydrophilic and Hydrophobic Segments

Sandeep Shukla,[1] A. K. Bajpai,[1] R. A. Kulkarni[2]

[1]*Bose Memorial Research Laboratory, Department of Chemistry, Government Autonomous Science College, Jabalpur (M.P.) 482 001, India*
[2]*Polymer Chemistry Division, National Chemical Laboratory, Pune (Maharashtra), India*

Received 8 September 2003; accepted 28 July 2004
DOI 10.1002/app.21344
Published online in Wiley InterScience (www.interscience.wiley.com).

ABSTRACT: The interpenetrating polymer network hydrogels based on poly(vinyl alcohol) were obtained by graft copolymerization of acrylamide and styrene onto polyvinyl alcohol in the presence of *N,N′*-methylene bisacrylamide as a crosslinking agent. The hydrogels were characterized by optical microscopy, scanning electron microscopy, infrared spectral analysis, differential scanning calorimeter, and thermogravimetric analysis. The hydrogels showed enormous swelling in aqueous medium and displayed swelling characteristics, which were highly dependent on the chemical composition of the hydrogels and pH of the swelling medium. The kinetics of water uptake and the mechanisms of water transport were studied as a function of composition of the hydrogel and pH of the swelling medium. © 2005 Wiley Periodicals, Inc. J Appl Polym Sci 95: 1129–1142, 2005

Key words: polyvinyl alcohol; IPN hydrogels; grafting; characterization; equilibrium swelling

INTRODUCTION

Hydrogels are three-dimensional networks of polymer chains that swell, but don't dissolve in water. The formation of hydrogels is an interesting phenomenon and could one day supplement tools for the design, synthesis, and self-assembly of novel biomaterials applications.[1–3] The particular suitability of hydrogels as biomaterials stems from the similarity of their physical properties to those of living tissues. This resemblance is due to their high water content, soft and rubbery consistency, and low interfacial tension. The high water content of hydrogel allows the extraction of undesirable reaction by-products prior to implantation and easy penetration of small molecules such as water, electrolytes, and metabolities into them *in vivo.* In addition to the use of hydrogels in implantation technology, they also find applications in controlled drug delivery systems,[4] soft contact lenses,[5] wound dressings,[3] artificial implants,[6] dialysis membrane,[7] surgical prostheses,[8] agrochemistry,[9] environmental monitoring,[10] etc. Their sensitive response to external stimuli such as pH,[11] temperature,[12] ionic strength,[13] magnetic field,[14] and electric field,[15] enable them to be coined "intelligent polymers" or "smart materials."

Correspondence to: A.K. Bajpai. E-mail: akbmrl@yahoo.co.in.

Journal of Applied Polymer Science, Vol. 95, 1129–1142 (2005)

Polyvinyl alcohol has been a polymer of choice for a long time in biotechnical and biomedical communities.[16–19] It is used as a basic material for a variety of biomedical applications including contact lenses,[20] skin replacement materials,[21] reconstruction of vocal cards,[22] artificial cartilage replacement,[23] artificial meniscus,[24] bioprosthetic heart valve,[25] etc., because of their inherent nontoxicity, noncarcinogenicity, good biocompatibility, and desirable physical properties such as elastic nature, high degree of swelling in aqueous solution, and good film forming property.[26] The polyvinyl alcohol has also gained wide pharmaceutical application as drug delivery matrices[24] or in the form of powders added to mixture of other excipients for tablet formation.[27] Despite all these, the main disadvantage of polyvinyl alcohol is its weak mechanical strength, although partial crystallization by annealing can increase the mechanical strength by 100-fold.[28]

The fundamental property to which all such biomedical applications are credited lies in swelling of the hydrogels when they come in contact with an aqueous environment.[29] A study of the dynamics of water sorption by hydrogel, therefore, is of much importance as it not only monitors the progress of swelling process, but also gives an insight into the mechanism of water transport, which reflects the network structure of hydrogel framework.[30] The use of hydrophobic segments into polymer matrix has also been attempted for altering physical properties of the polymer. In the present investigation, we report results on

the morphological and thermal characterization of a hydrogel composed of polyvinyl alcohol (PVA) and poly(acrylamide-co-styrene) or P(Am-co-ST) and its water uptake potential.

EXPERIMENTAL

Materials

PVA (hot processed M.Wt., 40,000; degree of hydrolysis, 98.6%) was obtained from Burgoyne Burbidges & Co. (Mumbai, India) and used without further purification. Acrylamide (AM) (Research Lab, Poona, India) was crystallized twice from methanol (G.R.) and dried under vacuum over anhydrous silica for a week. Styrene (Research Lab) was purified by washing it sequentially with 10% NaOH, 2 N H_2SO_4, and finally double distilled water. The monomer thus purified was distilled under vacuum conditions and middle fractions were collected. *N,N′*-Methylene bisacrylamide (MBA) (Central Drug House, Bombay, India) employed as a crosslinking agent and potassium persulfate (Loba Chemie, India) as polymerization initiators were used as received. All other chemicals used were of analytical grade and bidistilled water was used throughout the experiments.

Methods

Preparation of the IPN hydrogel

In the present study copolymerization of AM and styrene (ST) was carried out in the presence of both PVA and MBA. Prior to performing experiments, the reactants were degassed by purging dry N_2 for 60 min and then into a petri dish (diameter 2 inch, Corning) were added 1.00 g PVA, 10.5 mM AM, 8.6 mM ST, 0.12 mM MBA, and 1.11 M water. The reaction mixture was homogenized by manual mixing, deaerated again by purging N_2 gas for 1 h, and covered with a lid and kept at 80°C for 3 h. The interpenetrating polymer network (IPN) hydrogel so formed was dried at 60°C for 5 h.

Purification

The end-polymer networks obtained as described above were equilibrated with bidistilled water for 10 days so that the unreacted monomers and other reactants were leached out of the swollen IPN. Thereafter, the swelling medium was analyzed for acrylamide and styrene (unpolymerized double bond estimation), polyacrylamide, and polystyrene, respectively. It was found that whereas only 15% of monomers used were left unpolymerized, almost no homopolymers could be detected in the outer swelling medium. The swollen hydrogels were cut into small circular discs, which were then dried at room temperature for a week and stored in air-tight containers.

Grafting parameters

The percentage grafting yield and efficiency were calculated using the following equations.

$$\%\ \text{grafting yield} = \frac{(W_g - W_0)}{W_0} \times 100 \qquad (1)$$

$$\%\ \text{grafting efficiency} = \frac{(W_g - W_0)}{m} \times 100, \qquad (2)$$

where W_g, W_0, and m denote the weight of grafted PVA, the weight of ungrafted PVA, and weight of monomers (AM and ST) used, respectively.

The various samples, if prepared by taking different amounts of PVA, monomers (PVA and ST), and crosslinker (MBA) in the feed mixture, are listed in Table I. The % grafting yield and % grafting efficiency are also presented in Table I.

Appearance of the IPN hydrogel

In the dry state, IPN hydrogel was like a smooth thin film, which upon swelling changed into a semi-transparent enlarged mass as is evident from Fig. 1.

Morphology

Optical microscopy. The IPN film surface was examined by an optical microscope (NICON-E800 Eclipse) for morphological study.

Scanning electron microscopy. The surfaces of the IPN films were coated with Au-Pd under a vacuum and images were recorded with a Hitachi S-530 Scanning Electron Microscope at 10 kV and 3000× magnification.

IR spectra of semi-IPN hydrogels

The structural characterization of the IPN was performed by recording IR spectra of the end polymer on a Perkin–Elmer spectrophotometer (Paragon 1000 FTIR).

Thermal analysis

Differential scanning calorimetry

Differential scanning calorimetry (DSC) measurements were carried out on a TA instruments DSC-2C (Perkin–Elmer, Inc.) with nitrogen as purging gas. The experiments were performed from 50 to 400°C at a heating rate of 10°C/min.

TABLE I
Data Showing the Variation in Grafting Parameters with Varying Concentrations of Hydrogel Components

PVA (g)	AM (mM)	ST (mM)	MBA (mM)	Grafting efficiency (%)	Grafting yield (%)
0.250	10.5	8.6	0.12	27.50 ± 1.07	46.2 ± 1.42
0.500	10.5	8.6	0.12	29.32 ± 0.76	50.4 ± 1.53
0.750	10.5	8.6	0.12	29.85 ± 1.46	51.2 ± 1.09
1.000	10.5	8.6	0.12	30.07 ± 1.14	52.0 ± 1.11
1.250	10.5	8.6	0.12	31.78 ± 1.41	54.1 ± 1.17
1.500	10.5	8.6	0.12	33.54 ± 1.01	58.0 ± 1.11
1.000	7.00	8.6	0.12	17.57 ± 1.36	26.0 ± 1.16
1.000	10.5	8.6	0.12	30.07 ± 1.14	52.0 ± 1.11
1.000	14.0	8.6	0.12	42.00 ± 1.91	78.0 ± 2.23
1.000	17.6	8.6	0.12	52.48 ± 0.97	117.0 ± 3.64
1.000	21.1	4.3	0.12	54.00 ± 1.91	120.0 ± 2.23
1.000	24.6	8.6	0.12	57.00 ± 1.47	128.0 ± 1.11
1.000	10.5	2.1	0.12	43.00 ± 1.81	56.0 ± 1.47
1.000	10.5	4.3	0.12	48.00 ± 0.95	60.0 ± 2.16
1.000	10.5	8.6	0.12	30.07 ± 1.14	52.0 ± 1.11
1.000	10.5	13.0	0.12	23.15 ± 1.20	51.0 ± 2.06
1.000	10.5	15.1	0.12	20.02 ± 1.31	46.0 ± 1.80
1.000	10.5	17.3	0.12	16.50 ± 1.82	41.5 ± 1.45
1.000	10.5	8.6	0.06	32.96 ± 1.12	57.0 ± 1.80
1.000	10.5	8.6	0.12	30.07 ± 1.14	52.0 ± 1.11
1.000	10.5	8.6	0.19	27.10 ± 1.43	51.0 ± 2.38
1.000	10.5	8.6	0.25	35.85 ± 0.48	50.0 ± 1.80
1.000	10.5	8.6	0.32	22.00 ± 1.47	43.5 ± 3.14
1.000	10.5	8.6	0.39	17.50 ± 1.10	42.0 ± 1.47

Thermogravimetry analysis

Thermogravimetry analysis (TGA) was done on a TA instruments TGA-7 Perkin–Elmer thermogravimetry analyser with air atmosphere. Tests were conducted from 50 to 900°C at a heating rate of 10°C/min.

Swelling experiments

The progress of the swelling process was monitored gravimetrically as described by other workers.[31] In a typical swelling experiment, a preweighed circular piece of dry hydrogel (0.04 g) was immersed into a definite volume of bidistilled water, taken out at different time intervals, soaked between two filter papers, and finally weighed. The swollen ratio was calculated by the equation

$$\text{Swelling ratio} = \frac{\text{Weight of the swollen gel}}{\text{Weight of the dry gel}}. \quad (3)$$

Dynamics of water sorption

In order to have insights into the water transport process through the IPNs, the following equation was fit into the kinetic data of the swelling process,[32]

$$\frac{W_t}{W_\infty} = kt^n, \quad (4)$$

where k is the swelling rate front factor, n is the swelling exponent, and W_t and W_∞ are water intakes (g) at time t and equilibrium time (min), respectively. In the above equation the numerical value of n provides information about the water sorption mechanism, for example, for Fickian kinetics in which the rate of diffusion is rate limiting ($n = 0.5$), whereas the value of n between 0.5 and 1.0 indicates a non-Fickian process in which the relaxation of polymeric chains of the hydrogel determines the rate of water sorption. The value of n can be obtained from the double logarithmic plot drawn between W_t/W_∞ and time t.

For calculating the diffusion constant of water into the IPN, the following equation was employed,[33]

$$\frac{W_t}{W_\infty} = 4\left(\frac{Dt}{\pi\ell^2}\right)^{1/2}, \quad (5)$$

where D is the diffusion constant of water ($cm^2\ s^{-1}$) and ℓ is the thickness of the dry IPN measured by a micrometer.

Statistical analysis

All swelling experiments were performed four times and the swelling ratios were expressed as the average of three independent determinations. The values of percentage grafting yield and grafting efficiency are

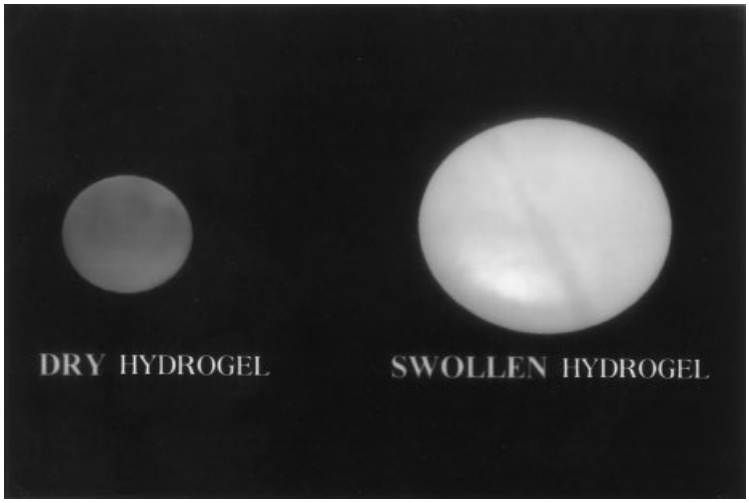

Figure 1 A photograph depicting the dry and swollen grafted hydrogels.

expressed as means ± S.D. of at least four independent measurements.

RESULTS AND DISCUSSION

Characterization of hydrogel

Morphology

A photograph of dry IPN hydrogel (Fig. 1) shows the homogeneous surface of semi-transparent film. An optical micrograph of the prepared dry hydrogel is depicted in Fig. 2, which clearly shows the presence of hydrophobic polymeric moieties due to the irregular location of polystyrene segments in the copolymeric chains of the network. The optical images also suggest that polystyrene segments are unevenly distributed over the film surface. The hydrogel was also analyzed by SEM analysis, which provides a better insight (Fig. 3) into the dimensions and morphology of the IPN hydrogels compared to that by an optical microscope. This image of film again confirms the predominant presence of hydrophobic microdomains on the hydrogel surface. These hydrophobic microdomains of polystyrene provide mechanical strength to the gel acting as reinforcement fillers and regulate the swelling behavior of the gel.

IR spectral analysis

The IR transmittance spectra of the end polymer is depicted in Fig. 4. The spectra clearly show a broad band around 3500 cm^{-1}, which is typical of hydrogen bonded (bridged) O—H stretch from alcoholic OH and bound water. The observed broad band also implies for N—H stretching due to polyacrylamide and MBA. Similarly, a strong amide I band at 1596 cm^{-1}

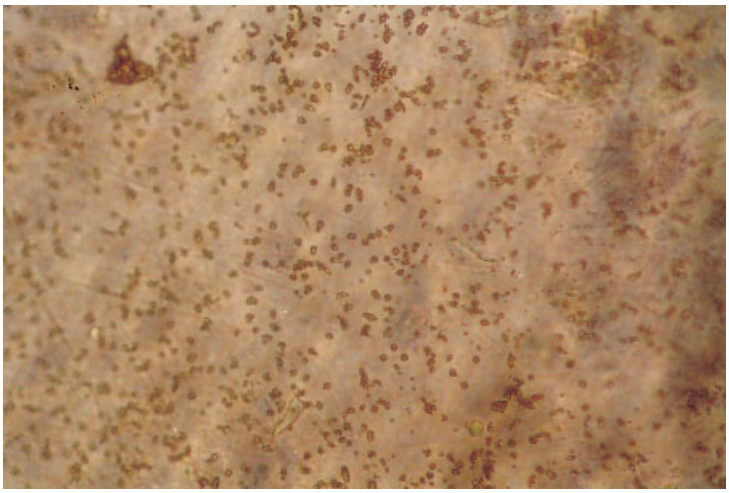

Figure 2 Optical micrograph of the dry grafted hydrogel.

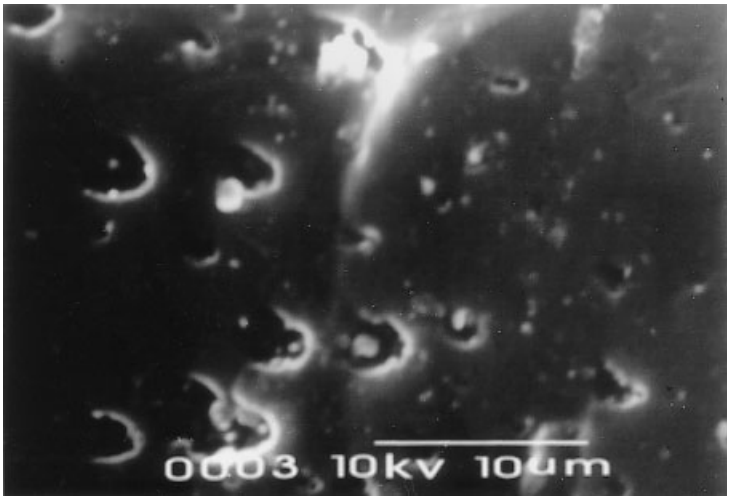

Figure 3 SEM image of the grafted hydrogel.

may also be assigned to C═O stretching vibration of polyacrylamide and MBA. The spectra also mark the presence of methylene (CH_2) twisting and wagging vibrations at 1361 and 1102 cm^{-1} and C—H stretching at 2933 cm^{-1}. In addition to the above-observed bands, the spectra also contain absorption bands in the range 1400 to 1500 cm^{-1} indicative of C═C skeletal in-plane vibrations due to the phenyl ring of styrene. The spectral analysis further suggests a grafted type of network structure in which crosslinked AM and ST chains are grafted onto the backbone of PVA via hydroxyls of the preformed polymer.

On the basis of the above spectral analysis, a scheme of reactions may be proposed for the formation of the IPN hydrogel as depicted in Fig. 5. The proposed scheme only explains the formation of the IPN chains:

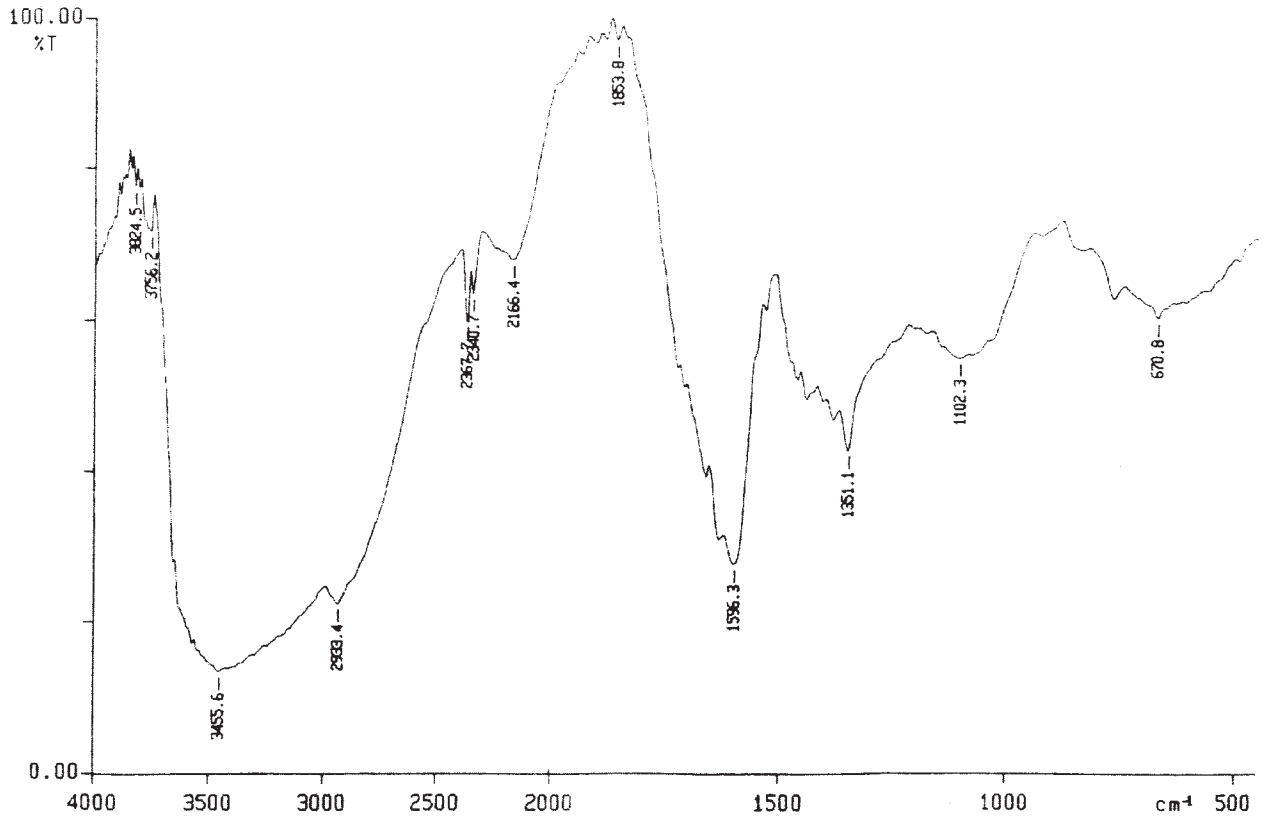

Figure 4 IR Spectra of the grafted hydrogels.

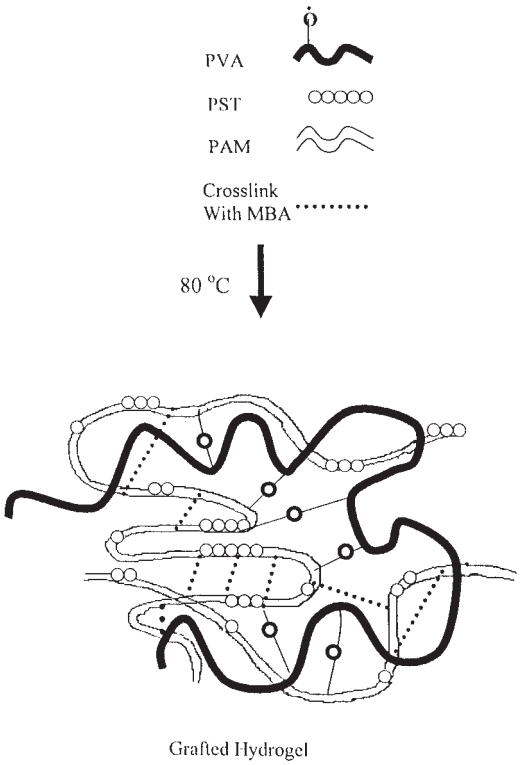

Figure 5 A proposed reaction scheme of mechanism for the synthesis of grafted hydrogels.

this does not indicate the formation of crystalline domains in the IPN.

Thermal analysis

For the assessment of thermal stability of the prepared hydrogels TGA and DSC studies were performed and the respective thermograms are shown in Figs. 6 and 7, respectively. It is clear from Fig. 6 that there is almost no weight loss up to 100°C, whereas a slight decomposition begins beyond 100°C, which could be assigned to the water loss in the hydrogel. The first major decomposition appears to occur at 164°C, which may be due to thermal processes involving both melting of polyacrylamide (PAM) chains and onset of degradation. This value, however, is comparatively low and may be attributed to the presence of other components in the hydrogel. In general, PAM shows three steps of weight loss located at 100, 200, and 340°C.[34] The former is attributed to moisture loss, the weight loss at 200°C is due to melting and decomposition, and the third drop at 340°C is indicative of the occurrence of more extensive thermal degradation processes. In the present case also, major decomposition starts at 335°C and continues up to 454°C; thereupon about

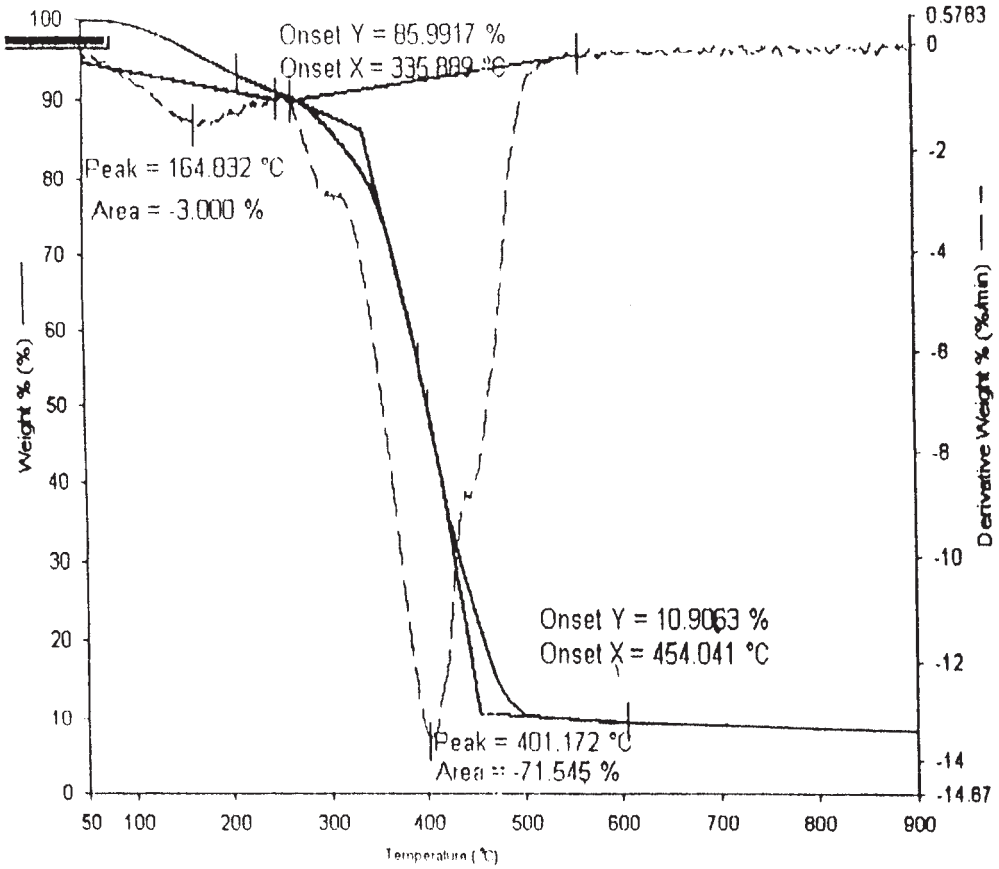

Figure 6 The TGA curves of grafted hydrogel of definite composition of [PVA] = 1.0 g, [AM] = 10.5 mM, [ST] = 8.6 mM, [MBA] = 0.12 mM, [KP] = 0.073 mM. Thickness = 0.051 cm; heating rate = 10°C/min.

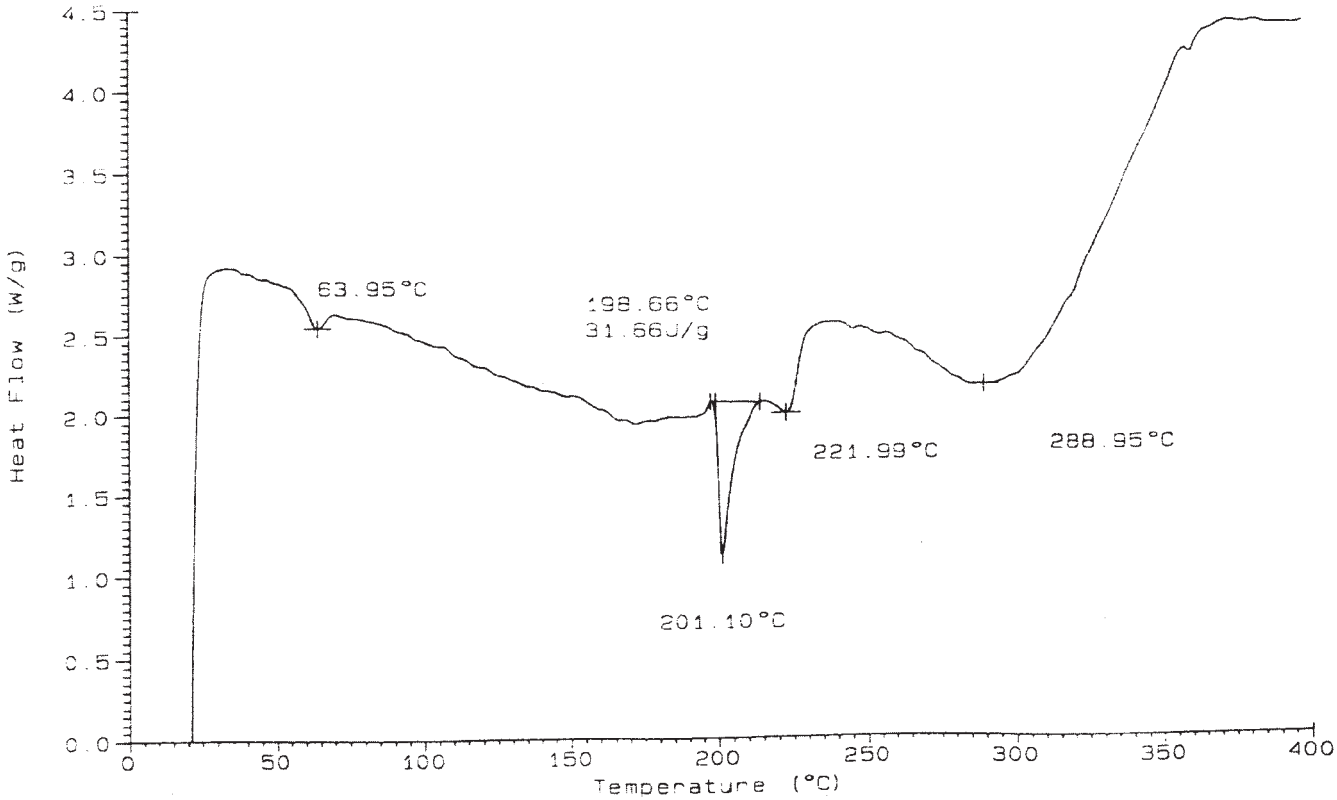

Figure 7 The DSC thermogram of grafted hydrogel of definite composition of [PVA] = 1.0 g, [AM] = 10.5 mM, [ST] = 8.6 mM, [MBA] = 0.12 mM, [KP] = 0.073 mM. Thickness = 0.051 cm; heating rate = 10°C/min.

75% weight loss is noticed. However, prominent decomposition occurs at 401°C as revealed by the TGA curves, which clearly show the greatest weight loss in the temperature range 250 to 450°C that is believed to be due to the disintegration of intermolecular and partial breaking of the molecular structure, as reported elsewhere.[35] A large peak area of 71% also suggests the presence of large crystalline domains in the hydrogel. The melting points of PVA and polystyrene (PST) also fall within the temperature range of 200 to 250°C so they were obscured in the TGA curves and did not appear separately.

The DSC thermogram shown in Fig. 7 clearly depicts a minor endotherm at 63°C, which could be assigned to the glass transition temperature of the PVA. A minor endotherm also appears near 165°C and may be attributed to the melting of PAM. The thermogram depicts a sharp melting endotherm at 198°C, which may be due to the melting of PST crystallite domains in the IPN. A high value of 31.66 J/g clearly suggests a higher crystallinity in the IPN. A broad but deep melting endotherm observed at 288°C may be because of melting of PVA semi-crystallite regions in the IPN. The thermogram contains broad and minor exotherms beyond 340°C that represent degradation of constituent polymers of the IPN.

Network parameters

Two important structural parameters characterizing crosslinked polymer are M_c, the average molar mass between crosslinks, and crosslink density (q), which may be determined by the equations,

$$M_c = -V_1 d_p \frac{(v_s^{1/3} - v_s)/2}{\ln(1 - v_s) + v_s + X v_s^2} \tag{6}$$

$$q = \frac{M_0}{M_c}, \tag{7}$$

where the terms involved have their usual significance.[36]

Other authors define a crosslink density, v_e, as the number of elastically affective chains, totally included in a network, per unit volume, v_e is simply related to q since

$$v_e = d_p N_A / M_c, \tag{8}$$

where N_A is Avogadro's number.

Since the IPN in the present study contains a copolymeric structure, the molar mass of the polymer repeat unit, M_0, can be calculated by the equation

TABLE II
Structural Parameters for the Networks of PVA and Poly(AM-*co*-ST) of Varying Compositions of the IPNs[a]

PVA (g)	AM (mM)	ST (mM)	MBA (mM)	Average mol. wt. between crosslinkers (M_c)	Crosslink density ($q \times 10^3$)	Elastically effective chains ($V_e \times 10^{-19}$)
1.000	7.00	8.6	0.12	20,204	4.24	3.57
1.000	10.5	8.6	0.12	79,399	1.08	0.91
1.000	17.6	8.6	0.12	21,322	3.83	3.38
1.000	10.5	4.3	0.12	34,607	2.32	2.08
1.000	10.5	8.6	0.12	79,399	1.08	0.91
1.000	10.5	13.0	0.12	21,318	4.18	3.39
1.000	10.5	8.6	0.06	110,625	0.75	0.65
1.000	10.5	8.6	0.12	79,399	1.08	0.91
1.000	10.5	8.6	0.25	15,949	5.38	4.53

[a] Structural parameters calculated for three different concentrations of AM, ST, and MBA.

$$M_0 = \frac{n_{AM} \cdot M_{AM} + n_{ST} \cdot M_{ST}}{n_{AM} + n_{ST}}, \quad (9)$$

where n_{AM} and n_{ST} are the mol. numbers of AM and ST (mol) and M_{AM} and M_{ST} are the molar mass of AM and ST (g mol-1), respectively.

The density of the polymer d_p was determined by pyknometry and found to be 1.2 g cm^{-3}. Other parameters such as V_1 and X were noted from the literature.[37,38] Using Eqs. (6), (7), and (8) the volumes of M_c, q, and v_e have been calculated for the IPNs containing different amounts of crosslinkers (MBA). The values summarized in Table II indicate that the average molar mass between crosslinks decreases with increasing MBA content in the networks.

Factors affecting grafting parameters

As shown in Table I the present grafting yield and grafting efficiency vary with varying composition of the hydrogel. The obtained grafting data may be interpreted as follows.

When the amount of PVA increases from 0.250 to 1.50 g, both the grafting yield and the grafting efficiency increase, which may be because increasing concentration of PVA results in increasing number of polymer radical, i.e., PVA, which obviously brings about an increase in grafting parameters.

In a similar way when the concentration of AM is varied in the range 7.0 to 24.60 mM, the grafting parameters constantly increase, which can be again explained on the basis of the proposed grafting mechanism. It is clear from the mechanism that increasing concentration of monomer (AM) increases the availability of monomer molecules in the propagation step and, therefore, the extent of grafting increases. However, an opposing trend is noticed when the concentration of hydrophobic monomer (styrene) is varied in the range 2.17 to 17.3 mM. The data clearly indicate a constant fall in both the grafting yield and the grafting efficiency. The observed decrease in grafting parameters may be because greater concentration of styrene may lead to the formation of homopolymer, which will result in a lower grafting yield and grafting efficiency. It is also likely that due to an increased hydrophobicity in the reaction mixture phase separation may also occur, which will lower the yield of grafted polymer.

It is also revealed by the data that increasing the concentration of crosslinker (MBA) results in a fall in both the percentage grafting yield and the grafting efficiency. The observed results may be explained by the fact that at higher concentration of crosslinking agent in the polymerization system, the greater number of crosslinker molecules add onto the active site on the PVA backbone rather than the monomers acrylamide and styrene.

Mechanism of water sorption

Polymeric hydrogels are normally considered either IPN, where different polymeric chains are held to one another via weak interactive forces, or intimate mixture of polymeric chains covalently bonded to one another. In the present work since the PVA and poly(acrylamide-co-styrene) chains offer a chemical interaction between themselves, the hydrogel synthesized may belong to the latter category. Thus, assuming the nature of the hydrogel as grafted copolymer, it can be postulated that there are free volume patches present between the PVA and copolymeric chains according to the free volume theory.[39] When the hydrogel contacts a thermodynamically compatible solvent the penetrant water molecules invade the hydrogel surface and, thus, a moving solvent front is observed that clearly separates the unsolvated glassy polymer region ahead of the front from the swollen and rubbery *IPN* phase behind it.[40] Just ahead of the front, the presence of solvent plasticizes the polymer and causes it to undergo a glass-to-rubber transition.[41] Now, the following possibilities arise:

(i) If the glass transition temperature of the polymer (T_g) is well below the experimental temperature, the polymer will be in the rubbery state and polymer chains will have a higher mobility that allows an easier penetration of the solvent.[42] This clearly results in a Fickian diffusion (Case I), which is characterized by a solvent diffusion rate, R_{diff}, slower than the polymer relaxation rate, R_{relax} ($R_{diff} \ll R_{relax}$).

(ii) If the experimental temperature is below T_g, the polymer chains are not sufficiently mobile to permit immediate penetration of the solvent into the polymer core. This gives rise to a non-Fickian diffusion process, which includes Case II diffusion and anomalous diffusion depending on the relative rates of diffusion and chain relaxation (for Case II, $R_{diff} \gg R_{relax}$, and for anomalous, $R_{diff} \sim R_{relax}$).

It has also been a matter of quest to know about the status of water molecules in the swollen hydrogel. It has been revealed by differential scanning calorimetry measurements[43] that water molecules are normally present in two different states in the hydrogel, viz. free water and bound water.

Effect of hydrogel composition on swelling

Macromolecular hydrogels generally consist of hydrophilic (and/or hydrophobic) components and a suitable crosslinking agent. Apart from the chemical functions of the hydrogels, the swelling of hydrogel network is also regulated by the physical forces and subsequent elastic responses of the constituent macromolecular chains of the matrix. According to Flory's swelling theory,[44] the following equation can be given,

$$Q^{5/3} = \left\{ \frac{[(i/2V_N \cdot S^{1/2}) + (1/2 - X_1)/V_1]}{(v_e/V_\sigma)} \right\}, \quad (10)$$

where i/V_N is the concentration of the fixed charge referred to unswollen network, S is ionic concentration in the external solution, $(1/2\text{-}X_1)/V_1$ is the affinity of hydrogel for water, and v_e/V_σ is the crosslinked density of the hydrogel. The above equation reveals that the swelling ratio has direct relations with ionic osmotic pressure, crosslinked density, and the affinity of hydrogel for water. Therefore, the swelling of the hydrogel can be controlled by varying its chemical composition.

Effect of styrene

An effective route to bring about the desired modification in the sorption property of a polymers is by introduction of a hydrophobic monomer into the hydrophilic system. This normally results in a change in the maximum hydration and diffusion of the swelling agent into the matrix as well as the organization of water molecules, depending on the chemical composition and the distribution of the hydrophobic monomeric units along the macromolecular chains.[45] For instance, the water gain property of a polymer of 2-hydroxylethyl methacrylate was affected by means of the introduction of a hydrophobic monomer such as furfurylacrylate.[46] Similarly, inclusion of a hydrophobic crosslinker into the polymer matrix has also been attempted for altering physical properties of the polymer.[47] The effect of increasing concentration of styrene on the equilibrium swelling behavior of hydrogel has been examined by varying its concentration in the range 2.17 to 17.3 mM in the feed mixture of the hydrogel. The results are displayed in Fig. 8, which indicates that with increasing proportion of styrene in the hydrogel, the equilibrium swelling of hydrogel increases up to 8.6 mM of styrene content, while beyond 8.6 mM a fall in equilibrium swelling of hydrogel is noticed. The observed initial increase in swelling of the gel may be explained by the fact that ST is hydrophobic and bulky. Moreover, its increasing concentration in the feed mixture results in a steric repulsion among the PST segments of the IPN chains, which widens the mesh size of the network pores and thus facilitates the penetration of water molecules. This obviously brings about an increased swelling of hydrogel.

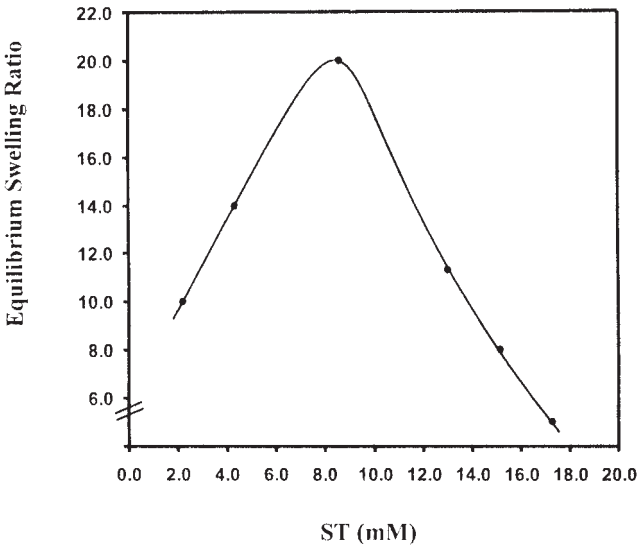

Figure 8 Effect of ST content on the equilibrium swelling of hydrogel at fixed composition of [PVA] = 1.0 g, [AM] = 10.5 mM, [MBA] = 0.12 mM, [KP] = 0.073 mM. Temperature = 27 ± 0.2°C; thickness = 0.051 cm; pH 7.0.

Effect of acrylamide

When the concentration of hydrophilic monomer, i.e., acrylamide, increases in feed mixture in the range 7.00

to 24.60 mM, initially equilibrium swelling of hydrogel increases, but after 10.5 mM there is a fall in the equilibrium swelling of hydrogel (Fig. 9). This may be explained by the fact that AM is a hydrophilic monomer and when the amount of AM increases the swelling of hydrogel also increases. However, after 10.5 mM the fall observed in the swelling of hydrogel could be attributed to the reason that further increasing AM concentration results in a greater density of the network, which obviously results in a drop in equilibrium swelling. Another reason for the observed decrease in swelling may be that with increasing hydrophilic segments in the hydrogel the polymer volume fraction decreases, which reduces the mesh sizes of the free volumes. The mesh size characterizes the space between the macromolecular chains. Obviously, a decrease in mesh size will result in a penetration of a smaller number of water molecules into the network.

Effect of PVA

When the concentration of PVA in the IPN varies in the range 0.25 to 1.5 g, the swelling ratio also changes appreciably (Fig. 10). Initially the swelling ratio increases, while in the latter course it constantly decreases. The results also reveal that at higher amounts of PVA, the equilibrium swelling is attained earlier in comparison to the hydrogel with low PVA content. The results can be explained by the fact that an increasing proportion of PVA results in a greater hydration of its chains because of the hydrophilic nature of the PVA. However, beyond an optimum concentration (1.0 g) the decrease observed in the swelling ratio is due to a much greater density of the gel, which inhibits diffusion of penetrant water molecules into the gel matrix. The arrival of the equilibrium swelling of hydrogel at earlier times at higher PVA concentration may be attributed to the fact that at higher PVA concentration relaxation of PVA chains becomes difficult and this obviously leads to much slower penetration of water molecules, which brings about an early arrival of equilibrium swelling of the hydrogels.

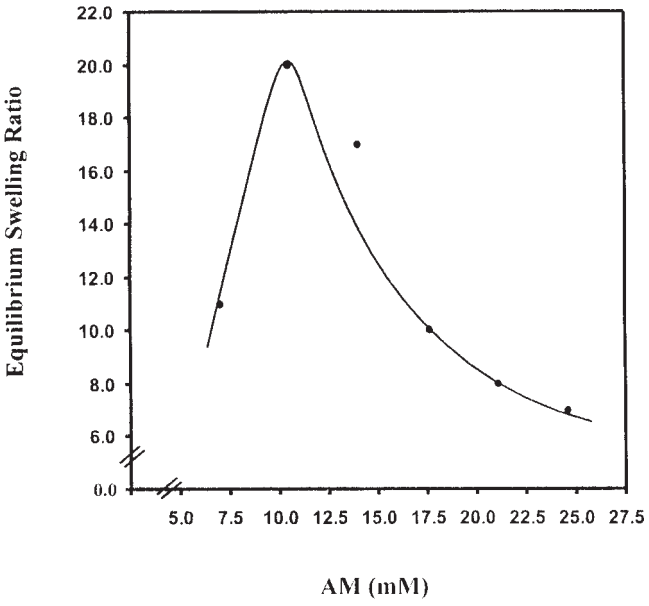

Figure 9 Effect of AM content on the equilibrium swelling of hydrogel at fixed composition of [PVA] = 1.0 g, [ST] = 8.6 mM, [MBA] = 0.12 mM, [KP] = 0.073 mM. Temperature = 27 ± 0.2°C; thickness = 0.051 cm; pH 7.0.

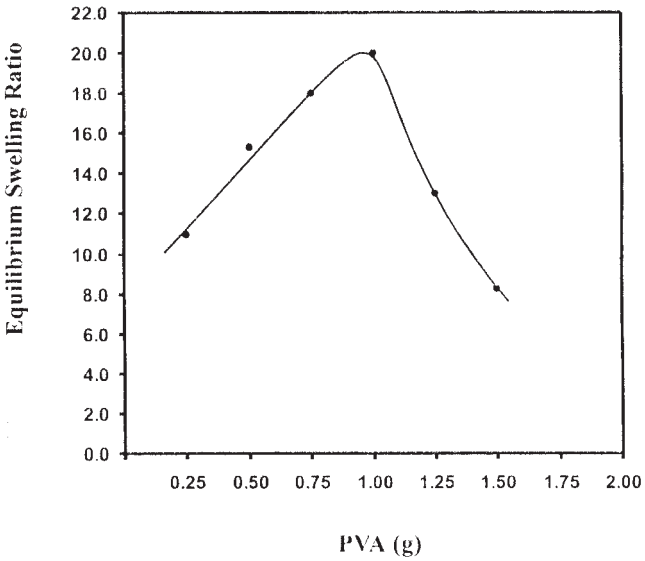

Figure 10 Effect of PVA content of the network on the equilibrium swelling of hydrogel for fixed composition of [ST] = 8.6 mM, [AM] = 10.5 mM, [MBA] = 0.12 mM, [KP] = 0.073 mM. Temperature = 27 ± 0.2°C; thickness = 0.051 cm; pH 7.0.

Effect of crosslinker

The influence of increasing crosslinking of the hydrogel on its release behaviour was investigated by employing different amounts of crosslinking agent (MBA) while in the network preparation. When MBA was used in the concentration range 0.06 to 0.39 mM in the feed mixture of the network, it was observed that whereas the equilibrium swelling increases up to 0.12 mM, concentration of MBA decrease in equilibrium swelling was noticed beyond 0.12 mM of crosslinker concentration (Fig. 11). The observed increase in equilibrium swelling may be attributed to these reasons. Since MBA is a hydrophilic monomer, its increasing concentration in the feed mixture results in an enhanced hydrophilicity of network, which in turn increases the degree of swelling. However, beyond 0.12 mM of MBA a significant decrease may be explained on the basis of the fact that crosslink density increases to appreciable extent; therefore, swelling of hydrogels decreases. It is clearly revealed in Table II that when

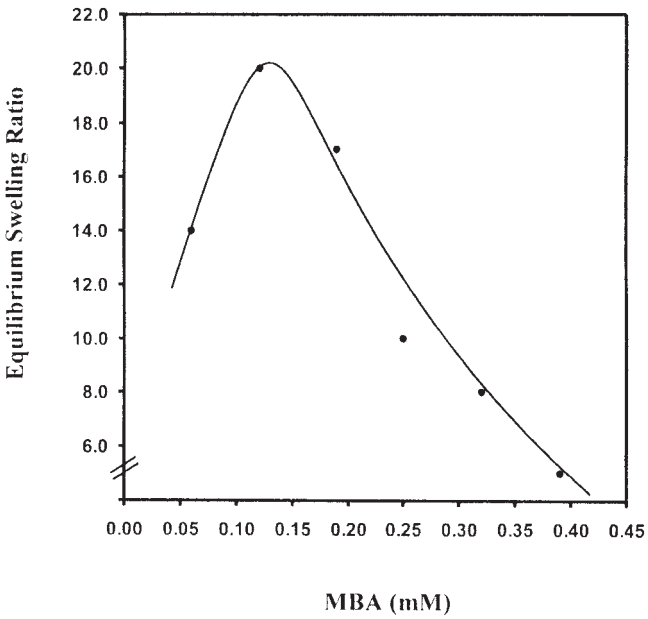

Figure 11 Effect of MBA content of the hydrogel on the equilibrium swelling of hydrogel at fixed composition of [PVA] = 1.0 g, [AM] = 10.5 mM, [ST] = 8.6 mM, [KP] = 0.073 mM. Temperature = 27 ± 0.2°C; thickness = 0.051 cm; pH 7.0.

the concentration of MBA increases from 0.06 to 0.12 mM, the crosslink density increases by 50%, whereas with a further increase in crosslink concentration, that is from 0.12 to 0.25 mM, the crosslink density increases by nearly 500%. Some authors[48] have reported an increase in the glass transition temperature (T_g) of the polymer with increasing concentration of the crosslinker. This also results in a restrained mobility of network chains and, therefore, slows the rate of swelling. As can be seen in Table III, the penetration velocity of the solvent also decreased with increasing concentration of the MBA; hence, this also supports the idea of slow penetration of water molecules into the hydrogel.

Effect of pH

The role of pH in regulating water sorption of polymeric hydrogels is of greater significance as a change in pH of the swelling medium often results in a fluctuation in free volumes accessible to penetrant water molecules, which, in turn, affects swelling characteristics of the polymer. In the present investigation, the effect of pH has been studied in the range 2.0 to 10.0 and the results are depicted in Fig. 12. It is clear that the equilibrium swelling increases with increasing pH of the swelling medium. This can be explained by the fact that with increasing pH of the swelling medium the polyacrylamide segments of the copolymer undergo partial hydrolysis and consequently produce anionic charged centers along the copolymeric chains. These polyelectrolyte chains cause repulsions between the macromolecular chains and thus widen the free volumes within the IPN network, which obviously enhances their water sorption quality.

It was also noticed from the kinetic swelling data (not given here) that at extreme pH's, i.e., 2.0 and 10.0, the equilibrium swelling arrives at earlier times than at other pH's. This can be explained by the fact that at extreme pH's of 2.0 and 10.0 the copolymeric chains will be most compactly and loosely packed, respectively, within the hydrogel and, therefore, there will be further no scope for polymeric chains to shrink or swell, respectively. This clearly leads to an earlier arrival of the equilibrium swelling.

TABLE III
Data Showing the Variation of Penetration Velocity (v) for Swelling of IPN and Diffusion Constant (D) with Varying Composition of the IPNs[a]

PVA (g)	ST (mM)	AM (mM)	MBA (mM)	Thickness (cm)	$v \times 10^5$ (cm/s)	$D \times 10^7$ (cm^2/s)
0.5	8.6	10.5	0.12	0.051	1.85	3.76
1.0	8.6	10.5	0.12	0.051	1.60	3.95
1.5	8.6	10.5	0.12	0.051	1.03	1.96
1.0	4.3	10.5	0.12	0.051	2.08	7.10
1.0	8.6	10.5	0.12	0.051	1.60	3.95
1.0	13.0	10.5	0.12	0.051	1.20	4.43
1.0	8.6	7.0	0.12	0.051	1.15	2.83
1.0	8.6	10.5	0.12	0.051	1.60	3.95
1.0	8.6	17.6	0.12	0.051	0.95	2.38
1.0	8.6	10.5	0.06	0.051	2.08	3.95
1.0	8.6	10.5	0.12	0.051	1.60	3.95
1.0	8.6	10.5	0.25	0.051	0.80	2.38
1.0	8.6	10.5	0.12	0.017	0.55	5.15
1.0	8.6	10.5	0.12	0.030	1.25	3.60
1.0	8.6	10.5	0.12	0.051	1.60	2.56

[a] Values calculated for three different concentrations of PVA, ST, AM, and MBA.

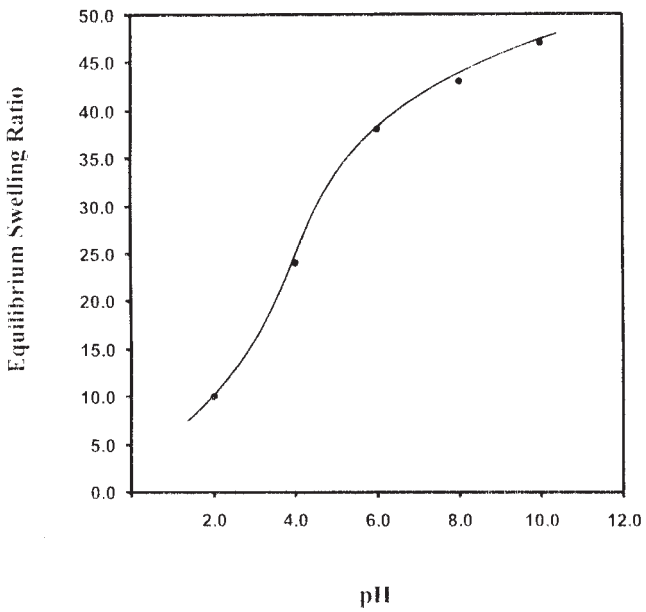

Figure 12 Effect of pH of swelling medium on equilibrium swelling at fixed composition of [PVA] = 1.0 g, [AM] = 10.5 mM, [ST] = 8.6 mM, [MBA] = 0.12 mM, [KP] = 0.073 mM. Temperature = 27 ± 0.2°C; thickness = 0.051 cm.

Effect of thickness

In the present study, the influence of surface area of the hydrogels on the swelling kinetics has been studied by varying the thickness of hydrogels in the range 0.017 to 0.051 cm. The results are shown in Fig. 13, which indicates that the equilibrium swelling increases with increasing thickness of the hydrogel. Initially, thinner gels show higher swelling but attained equilibrium swelling earlier compared to a thicker gel. Because of the thicker hydrogel, greater force will be required to stretch it, as evident from the equilibrium swelling of the thickest gel (0.051 cm). The degree of swelling of a hydrogel is controlled by a combination of free energies of mixing between water and the hydrophilic polymer chains and by the elastic response of the rubbery network to the expansion due to water uptake. Similar type of results have been reported by other workers.[49]

Analysis of kinetic data

The swelling exponent (n) evaluated from EQ. (4) is of great significance in looking into the mechanistic insights of the water-transport mechanisms. The data summarized in Table IV for definite concentrations of the hydrogel components, may be explained as follows.

When the PVA content of the hydrogel varies from 0.5 to 1.5 g, a shift in sorption mechanism is noticed from Fickian to anomalous, thus indicating that an increased number of PVA chains causes a widening of the mesh size of the gel and this, in turn, increases the rate of diffusion of water molecules. This clearly explains the equality of rates of diffusion of water molecules and network chain relaxation (i.e., $R_{diff} \sim R_{relax}$), which causes an anomalous type of mechanism.

Variation in the hydrophobic monomer (styrene) in the hydrogel in the range 4.3 to 13.0 mM results in a shift of transport mechanism from anomalous to Super Case II. The data indicate that in the concentration range 4.3 to 8.6 mM, the relative rates of diffusion and chain relaxation are almost equal ($R_{diff} \sim R_{relax}$); however, at much higher concentration of styrene hydrophobic repulsion and steric hinderance cause an overrelaxation of network chains, thus producing a Case II mechanism.

When hydrophilic monomer (acrylamide) varied in the range 7.0 to 17.6 mM, the water-sorption mechanism remains anomalous in nature, thus suggesting that the relative rates of diffusion of water molecules and chain relaxation remain almost identical in the studied range and introduction of hydrophilic monomer does not influence the swelling mechanism.

The effect of crosslinker (MBA) on the swelling mechanism has been studied by varying its concentration in the range 0.06 to 0.25 mM. The results summarized in Table IV clearly indicate the water-sorption mechanism changes from Fickian to anomalous type. The observed change in mechanism is quite obvious as, with increasing number of crosslinks in the hydrogel, the rate of chain relaxation slows and becomes almost comparable to that of diffusion of water mol-

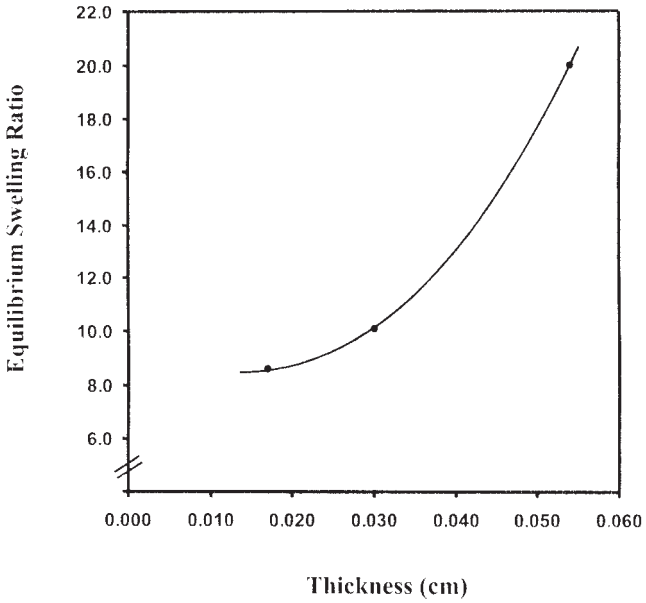

Figure 13 Effect of thickness of the hydrogel on the equilibrium swelling at fixed composition of [PVA] = 1.0 g, [AM] = 10.5 mM, [ST] = 8.6 mM, [KP] = 0.073 mM. Temperature = 27 ± 0.2°C; pH 7.0.

TABLE IV
Data Showing the Variation of Diffusional Exponent *n* with Varying Composition of the IPNs[a]

PVA (g)	ST (mM)	AM (mM)	MBA (mM)	Thickness (cm)	*n*	Swelling mechanism
0.5	8.6	10.5	0.12	0.051	0.46	Fickian
1.0	8.6	10.5	0.12	0.051	0.80	Anomalous
1.5	8.6	10.5	0.12	0.051	0.60	Anomalous
1.0	4.3	10.5	0.12	0.051	0.80	Anomalous
1.0	8.6	10.5	0.12	0.051	0.80	Anomalous
1.0	13.0	10.5	0.12	0.051	1.20	Super Case II
1.0	8.6	7.0	0.12	0.051	0.66	Anomalous
1.0	8.6	10.5	0.12	0.051	0.80	Anomalous
1.0	8.6	17.6	0.12	0.051	0.60	Anomalous
1.0	8.6	10.5	0.06	0.051	0.58	Fickian
1.0	8.6	10.5	0.12	0.051	0.80	Anomalous
1.0	8.6	10.5	0.25	0.051	0.66	Anomalous
1.0	8.6	10.5	0.12	0.017	0.48	Fickian
1.0	8.6	10.5	0.12	0.030	0.62	Anomalous
1.0	8.6	10.5	0.12	0.051	0.80	Anomalous

[a] Values calculated for three different concentrations of PVA, ST, AM, and MBA

ecules, thus resulting in an anomalous transport mechanism.

Similarly, a variation in thickness of hydrogel from 0.017 to 0.051 cm results in a shift from Fickian to anomalous type, which implies that at the lowest thickness the swelling was diffusion controlled, while at higher thickness the diffusion and relaxation rates become almost equal. The results are expected and may be explained by the fact that, with increasing thickness of the gel, the relaxation of macromolecular chains becomes slower and the two rates become almost identical, i.e., $R_{diff} \sim R_{relax}$.

CONCLUSION

Grafting of acrylamide and styrene onto polyvinyl alcohol in the presence of a crosslinking agent (MBA) results in a hydrogel with enormous water sorption capacity. Whereas the IR spectral analysis suggests a grafted type of network, its morphological study indicates an uneven distribution of hydrophobic polystyrene segments in the hydrogel network. The thermal analysis suggests a major decomposition between 250 and 450°C.

The prepared hydrogel displays a large water-absorbing capacity, which is greatly affected by its chemical architecture. A variation in styrene, acrylamide, PVA, and crosslinker (MBA) concentrations in the feed mixture of the hydrogel brings about an increase in water sorption capacity, while at higher concentrations of the added hydrogel components a fall in the swelling ratio is noticed.

The swelling property of grafted hydrogel is also influenced by varying pH of the medium (2.0 to 10.0) and a constant increase in the swelling ratio is observed with increasing pH of the swelling bath. The hydrogel also attains equilibrium swelling values at relatively earlier times at extreme acidic and alkaline pH. The water sorption capacity of the hydrogel is also dependent on the thickness of the swelling material and the extent of water uptake increases with increasing thickness of the hydrogel.

Acknowledgments

The authors gratefully acknowledge the financial assistance rendered to them by the Department of Science and Technology, New Delhi (India), in the form of Major Research Project No. SP/S1/G-11/2001.

References

1. Laporete, R. J. Hydrophilic Polymer Coating for Medical Devices: Technoic: Lancaster, PA, 1997.
2. De, D. R.; Kajiwara, K.; Osada, Y.; Yamauchi, A. Polymer Gel: Fundamental and Biomedical Applications; Plenum Press: New York, 1991.
3. Rosiak, J. M.; Ulanski, P.; Pajewski, L. A.; Yoshii, F.; Makuuchi, K. Radiat Phys Chem 1995, 46(2), 161.
4. Peppas, N. A. Curr Opin Colloid Interface Sci 1997, 2, 531.
5. Chirila, T. V.; Constable, I. J.; Crawford, G. J; Vijayasekaran, S.; Thompson, D. E.; Chen, Y. C.; Fletcher, W. A.; Griffin, B. J. Biomateries 1993, 14, 26.
6. Jeyanthi, R.; Rao, K. P. Biomaterials 1990, 11, 238.
7. Ikada, Y. Polym J 1991, 23, 551.
8. Williams, D. F. In Concise Encyclopedia of Medical and Dental Materials; Pergamon Press: Oxford, England, 1990.
9. Saragdin, D.; Karadag, E.; Guven, O. Polym Bull 1998, 41, 577.
10. Rivas, B. L.; Maturana, H. A.; Pereira, E. Angew Makromol Chem 1994, 220, 61.
11. Snowden, M. J.; Chowdhury, B. Z.; Vincent, B.; Morris, G. E. J Chem Soc Faraday Trans 1996, 92(24), 5013.
12. Bae, Y. H.; Okano, T.; Kim, S. W. J Polym Sci Polym Phys 1990, 28, 923.
13. Siegal, R. A.; Firestone, B. A. Macromolecules 1988, 21, 3254.
14. Mayer, C. R.; Cabail, V.; Lalot, T.; Thouvenot, R. Adv Mater 2000, 6, 12.

15. Kim, S. Y.; Shin, H. S.; Lee, Y. M.; Jeong, C. N. J Appl Polym Sci 1999, 73, 1675.
16. Ruiz, J.; Mantecon, A.; Cadiz, V. J. Appl. Polym. Sci. 2002, 85(8), 1644.
17. Hyon, S. H.; Cha, W. I.; Ikada, Y.; Kita, M.; Ogura, Y.; Honda, Y. J Biomater Sci Polym Ed 1994, 5, 397.
18. Juang, J. H.; Baoner, W. S.; Ogawa, Y. J.; Vacanti, P.; Weir, G. C. Transplantation 1996, 6, 1557.
19. Peppas, N. A.; Yang, W. H. Proc IUPAC 1980, 27, 28.
20. Charadack, W. M.; Brueske, D. A.; Santomauro, A. P.; Fazekas, G. Ann Surg 1962, 155, 127.
21. Peppas, N. A.; Benner, R. E. Jr. Biomaterials 1980, 1, 158.
22. Peppas, N. A. Biomater Med Dev Artif Org 1974, 7, 421.
23. Masuda, M. In Polyvinyl Alcohol; Finch, C. A., Ed.; Wiley: New York, 1992.
24. Kobayashi, M.; Toguchida, J.; Oka, M. Biomaterials 2003, 24, 639.
25. Wan, W. K.; Campbell, G.; Zhang, Z. F.; Hui, A. J.; Boughner, D. R. J Biomed Mater Res (Appl Biomater) 2002, 63, 854.
26. Thanoo, B. C.; Sunny, M. C.; Jayakrishanan, A. J Pharm Pharmacol 1993, 45, 16.
27. Corstensen, J. T.; Marty, J. P.; Puisiex, F.; Fessi, H. J Pharmacol Sci 1981, 70, 222.
28. Peppas, N. A.; Merrill, E. W. J Polym Sci Polym Chem Ed 1976, 14, 441.
29. Tighe, B. J. In Hydrogels in Medicine and Pharmacy; Peppas, N. A. Ed.; CRC Press: Boca Raton, FL, Vol III, 1987.
30. Wang, C.; Li, Y.; Hu, Z. Macromolecules 1997, 30, 4727.
31. Bajpai, A. K.; Srivastava, M. J Sci Ind Res 2001, 60, 131.
32. Bernus, A. R.; Hopfenberg, H. B. Polymer 1978, 19, 489.
33. Crank, J. In Mathematics of Diffusion; Clarendon Press: Oxford, 1978; p. 239.
34. Freddi, G.; Tsukada, M.; Beretta, S. J Appl Polym Sci 1999, 71, 1653.
35. Hirabayashi, K.; Suzuki, T.; Nagura, M.; Ishikawa, H. Bunseki K. 1974, 12, 437.
36. Ding, Z. Y.; Akinois, J. J.; Saloyev, R. J. Polym Sci Polym Phys 1991, 20, 1035.
37. Rosiak, J.; Burezak, K.; Czolzynaka, T.; Pekalu, W. Radiat Phys Chem 1983, 917, 22.
38. Hooper, H. H.; Baker, J. P.; Blanch, H. W.; Prausnitz, J. M. Macromolecules 1990, 23, 1096.
39. McNeil, M. E.; Graham, N. B. J Biomater Sci Polym Ed 1996, 7, 953.
40. Allroy, I.; Gurnor, E. F.; Lloyd, W. G. J Polym Sci 1966, C12, 249.
41. Thomas, N. L.; Wintle, A. H. Polymer 1980, 21, 613.
42. Grinsted, R. A.; Clark, L.; Koenig, J. L. Macromolecules 1992, 25, 1235.
43. Plathe, F. M. Macromolecules 1998, 31, 6721.
44. Flory, P. J. In Principles of Polymer Chemistry, Corner University Press: New York, 1953.
45. Vozquez, B.; Roman, J. S.; Peniche, C.; Cohen, M. E. Macromolecules 1997, 8440, 30.
46. Peniche, C.; Zaldivar, D.; Gallardo, A.; San Roman J. J Appl Polym Sci 1994, 54, 959.
47. Peniche, C.; Cohen, M. E.; Vazquez, B.; San Roman, J. J Polymer 1977, 38, 5677.
48. Ramraj, B.; Radhakrishanan, G. Polymer 1994, 35(10), 2167.
49. McNell, M. E.; Graham, N. B. J Biomater Sci Polym Ed 1993, 5(1/2). 111.